

# An Inverse Boundary Element Method for Determining the Hydraulic Conductivity in Anisotropic Rocks

R. Mustata<sup>1</sup>, S. D. Harris<sup>2</sup>, L. Elliott<sup>1</sup>, D. Lesnic<sup>1</sup>, D. B. Ingham<sup>1</sup>

**Abstract:** An inverse boundary element method is developed to characterise the components of the hydraulic conductivity tensor  $\mathbf{K}$  of anisotropic materials. Surface measurements at exposed boundaries serve as additional input to a Genetic Algorithm (GA) using a modified least squares functional that minimises the difference between observed and BEM-predicted boundary pressure and/or hydraulic flux measurements under current hydraulic conductivity tensor component estimates.

**keyword:** Boundary Element Method, Genetic Algorithms, inverse problems, anisotropy, hydraulic conductivity.

## 1 Introduction

The production of gas and oil in many reservoirs is seriously affected by their highly heterogeneous and/or anisotropic structure. From the fluid flow point of view, it is well accepted that heterogeneity and anisotropy are two closely related properties. Inhomogeneous materials are usually thought to appear homogeneous, but anisotropic, when considered at a scale much larger than the largest scale of heterogeneity.

The origin of anisotropy in rocks was discussed by Lake (1988) from the transport properties point of view. One conclusion is that the directionality of the pore structure, namely the preferred orientation of the microcracks or of non-spherical grains, can only produce moderate hydraulic conductivity anisotropy (experimental evidence was given by Rice, Fontugne, Latini, and Barduhn (1970)). Strong hydraulic conductivity anisotropy is more likely to originate from fine-scale heterogeneities in such materials as, for example, sand-shale sequences, aeolian deposits and jointed or fractured rock masses. As a consequence, it can be stated that anisotropy, like heterogeneity, is scale dependent (see Dagan (1986)). The scaling-up of the hydraulic conductivity from the centimetre-scale, as in cores or well logs, to the scale of hundreds of metres, such as grid blocks in large-scale numerical simulations, is a problem which is often encountered by reservoir engineers. Many techniques have been proposed to perform this task, more commonly known as determining grid block effective hydraulic conductivities. However, difficulties are

often encountered, especially in the case of multiphase flow (see Hewett and Behrens (1990)). The fundamental equation describing fluid flow in porous media, namely Darcy's Law, is itself the result of such a scaling process, from pore to sample scale. The difficulty that remains is to demonstrate that the coefficient of proportionality thus obtained, namely the hydraulic conductivity, is a material property, i.e. it is independent of the boundary conditions. Similarly, to be valid, the scaled-up, or effective, hydraulic conductivities should not depend on the boundary conditions. It is commonly believed that this requirement is automatically satisfied if the spatial domain considered, i.e. the grid block, is much larger than the largest scale of the heterogeneity contained in it, so that the material can be considered globally homogeneous (see for example, Begg, Carter, and Dranfield (1989)).

In this paper, the steady state flow of a single liquid phase through a rectangular, two-dimensional piece of homogeneous, anisotropic material is analysed using a BEM approach. This particular geometry has been chosen since it corresponds to the configuration traditionally employed in laboratory measurements. A GA based inverse technique is employed for the identification of the components of the hydraulic conductivity tensor using additional pressure and/or hydraulic flux values at the exposed boundaries.

## 2 Mathematical Formulation

In this section we consider an anisotropic medium in an open domain  $\Omega \subset D^d$ , where  $d$  is the dimension of the space in which the problem is posed, usually  $d \in \{1, 2, 3\}$ , and we assume that  $\Omega$  is bounded by a surface  $\Gamma$  which may consist of several segments, each being sufficiently smooth in the sense of Liapunov (see for example Sternberg and Smith (1946)). One way to deal with the anisotropy is to transform the governing differential equation into its canonical form by changing the spatial coordinates. However, after the transformation the boundary conditions are often more complicated than the original ones. Therefore, rather than using this approach we derive the fundamental solution required in the solution procedure for the differential operator in its original form.

If the influence of gravity is neglected, then Darcy's law is most frequently formulated as follows

$$\underline{Q} = -\frac{k}{\mu} \nabla p \quad (1)$$

<sup>1</sup> Department of Applied Mathematics University of Leeds, Leeds, LS2 9JT, UK, Tel: +44 (0)113 233 5113.

<sup>2</sup> Rock Deformation Research, School of Earth Sciences, University of Leeds, Leeds, LS2 9JT, UK, Tel: +44 (0)113 233 5252.

where  $\underline{Q}$  is the macroscopic flux rate, i.e. the volume of fluid crossing a unit area per unit time,  $k$  is the scalar permeability,  $\mu$  is the fluid viscosity and  $p$  is the macroscopic fluid pressure. Eq. 1 corresponds to one-dimensional flow in that  $\underline{Q}$  and  $\nabla p$  are collinear and, consequently, only one space variable is required. Clearly Eq. 1 applies only to isotropic porous materials since, by definition,  $k$  does not depend on the flow direction. An important experimental result is that Eq. 1, the scalar (or one-dimensional) form of Darcy's law, has been observed to hold in isotropic media provided that laminar flow conditions prevail, i.e. low Reynolds numbers.

In the case of anisotropic materials, a generalised form of Darcy's law has been suggested in which the tensor form of the permeability is represented as a positive definite symmetric tensor  $\mathbf{K}$ . The components of  $\underline{Q}$  are then written as follows

$$Q_i = - \sum_{j=1}^d \frac{k_{ij}}{\mu} \frac{\partial p}{\partial x_j} \quad \text{for } i = \overline{1, d} \quad (2)$$

where  $k_{ij}$  represents the components of the tensor  $\mathbf{K}$ . It should be noted that in the rest of this paper we consider only the two-dimensional case, i.e.  $d = 2$ , and therefore the components of  $\mathbf{K}$  in a given reference frame  $x_1, x_2$  are indicated by  $k_{11}, k_{12} = k_{21}, k_{22}$ .

The governing equation for single-phase flow in a two-dimensional anisotropic, homogeneous, porous medium can be derived from Darcy's law and the conservation of mass to produce the following form

$$\sum_{i,j=1}^2 k_{ij} \frac{\partial^2 p}{\partial x_i \partial x_j} = \mu \Phi_s \frac{\partial p}{\partial t} \quad \text{for } (x_1, x_2) \in \Omega \quad (3)$$

where  $t$  is the time and  $\Phi_s$  is the effective fluid storage capacity, i.e. the volume of fluid which must be injected or released from a unit volume of rock to cause a unit pressure change. The physical properties of the rock are assumed to be constant, and therefore the coefficients  $k_{ij}$  are independent of both space and time variables. Clearly, for the case in which  $k_{ij} = k \delta_{ij}$ , where  $\delta_{ij}$  is the Kronecker delta symbol, we obtain the isotropic situation.

In the following sections we investigate the steady state case, i.e.  $p$  is independent of time, and we discuss problems associated with the equation

$$\sum_{i,j=1}^2 K_{ij} \frac{\partial^2 p}{\partial x_i \partial x_j} = 0 \quad \text{for } (x_1, x_2) \in \Omega \quad (4)$$

which are distinct with respect to the imposition of the conditions on the boundary  $\partial\Omega = \Gamma = \bigcup_{l=0}^M \Gamma_l$ , where  $\Gamma_l \neq \emptyset$  do not intersect one another and have a smooth common boundary. In the above formulation  $K_{ij}$  are the coefficients of the hydraulic conductivity tensor defined as

$$K_{ij} = \frac{\gamma_w k_{ij}}{\mu}, \quad i, j = 1, 2 \quad (5)$$

where  $\gamma_w$  is the specific weight of the fluid.

## 2.1 Direct Problem

For direct, steady-state, elliptic problems, such as those governed by the steady state diffusion equation as given by Eq. 4, the boundary conditions are usually linear and of the Robin type, namely

$$c_l p(\underline{x}) + d_l \frac{\partial p}{\partial \mathbf{v}^+}(\underline{x}) = f_l(\underline{x}) \quad \text{for } \underline{x} \in \Gamma^l \quad l = \overline{0, M} \quad (6)$$

where

$$\frac{\partial}{\partial \mathbf{v}^+} = \sum_{i,j=1}^2 K_{ij} \cos(\mathbf{v}^+, x_i) \frac{\partial}{\partial x_j}, \quad i, j = 1, 2 \quad (7)$$

$c_l$  and  $d_l$  are prescribed constants,  $f_l$  are known functions of  $\underline{x}$  for  $l = \overline{0, M}$  and  $\cos(\mathbf{v}^+, x_i)$  are the direction cosines of the positive normal  $\mathbf{v}^+$  to the surface  $\Gamma$ . In the boundary conditions 6, the coefficients  $c_l$  and  $d_l$  are considered to be either zero or unity, thus incorporating the boundary conditions of both the Dirichlet and the Neumann type. In this direct formulation, the boundary conditions are assumed to be known while the distribution of the unknown function  $p$  within the domain is sought. The solution of the direct, well-posed problem for the steady state equation in an anisotropic media is obtained by employing a direct boundary integral equation method in which the fundamental Green's function of the associated differential operator to Eq. 4 and Green's second formula are used to reformulate the partial differential equation as an integral equation.

## 3 Boundary Element Solution for the Direct Problem

A classical boundary integral equation method, see for example Symm and Pitfield (1974) or Brebbia, Telles, and Wrobel (1984), is used in order to solve the direct, well-posed problem given by Eq. 4 and the boundary conditions 6. Since all the numerical approximations take place only at the boundaries, the dimensionality of the problem is reduced by one and a smaller system of equations is obtained in comparison to those achieved through finite-difference and finite element methods. Thus, there is a significant advantage in reducing the governing partial differential equation to an integral equation since the numerical solution of the integral equation requires less computational effort. The boundary integral approach is particularly suitable for irregular domains with complicated boundary conditions, being widely accepted as a useful method for both direct and inverse problems.

## 4 Model Validation

In order to illustrate the technique employed in this paper both the direct and inverse problem are solved in the plane square domain  $\Omega = [0, 1] \times [0, 1]$ , corresponding to the case  $M = 3$  in

Eq. 6. Further, we consider the differential operator  $\mathbf{L}$  given by

$$\mathbf{L}p(x_1, x_2) = \frac{\partial^2 p}{\partial x_1^2} + \frac{\partial^2 p}{\partial x_1 x_2} + \frac{\partial^2 p}{\partial x_2^2} \quad (8)$$

which defines the diffusion equation, namely Eq. 4, in an anisotropic porous medium when the hydraulic conductivity tensor  $\mathbf{K}$  is chosen to have the components  $K_{11} = K_{22} = 1.0$  and  $K_{12} = K_{21} = 0.5$ . The analytical pressure distribution to be retrieved is given by

$$p(x_1, x_2) = x_1^2 - 4x_1x_2 + x_2^2 \quad (9)$$

The most significant quantity to characterise the anisotropy of the medium is the determinant of the hydraulic conductivity matrix, i.e.  $\det(\mathbf{K}) = K_{11}K_{22} - K_{12}^2$ . The smaller the value of  $\det(\mathbf{K})$ , the more asymmetrical are the pressure field and the hydraulic flux vectors. Since the criterion  $\det(\mathbf{K}) > 0$  determines the type of differential equation, parabolic for transient problems and elliptic for steady problems, the smaller the value of  $\det(\mathbf{K})$ , the more difficult are the numerical calculations. Thus, in order to maintain reasonable accuracy, the determinant of the hydraulic conductivity matrix must not be too small, see Chang, Kang, and Chen (1973).

#### 4.1 Direct Problem

In the direct formulation for the test example 9, a boundary element method using 40, 80 and 160 boundary elements is employed in order to provide simultaneously the unspecified boundary pressures and hydraulic fluxes. Once these quantities have been obtained accurately, the pressure distribution inside the sample can be determined by simple numerical integration using the integral form associated with the governing partial differential equation. Various types of boundary condition formulations of the direct problem can be employed to illustrate the method and to investigate its accuracy with respect to increasing the number of boundary elements.

Once the values of the hydraulic flux and pressure on the boundaries have been obtained with reasonable accuracy, the boundary element method can be used explicitly to determine the pressure distribution inside the domain. If we consider the numerical solution obtained using 40, 80 and 160 boundary elements at the single point  $(x_1, x_2) = (0.5, 0.5)$  then we find that the exact solution is approximated with an error which is less than 0.16%, 0.01% and 0.003%, respectively, and similar results are obtained at any arbitrary point in the solution domain.

#### 4.2 The Inverse Problem Formulation

The inverse analysis requires the identification of the components of the hydraulic conductivity tensor only from measurements of the pressure and/or hydraulic flux on the boundary of the rock sample. Internal measurements within the rock

sample are to be avoided if the sample is not to be damaged. Therefore, we must retrieve the three unknowns, namely  $K_{11}$ ,  $K_{12}$  and  $K_{22}$ , from the same number of independent additional measurements of the available boundary information, namely the pressure or hydraulic flux, which is the minimum necessary condition for identifiability.

##### 4.2.1 Sensitivity Coefficients and Ratios

Prior to performing the inverse analysis, it is useful to calculate the sensitivity coefficients as a function of time. Sensitivity coefficients provide indicators of the suitability of the design of the experiment and, in general, they are desired to be uncorrelated. For this situation, i.e. the steady state case, these coefficients take the form of the boundary pressure and/or hydraulic flux response to small changes in the coefficients of the hydraulic conductivity tensor. We can use the sensitivity coefficients to determine the optimal data measurements to be imposed or recorded in order to reduce the ill posedness of the inverse formulated problem. The normalised sensitivity coefficients, as a function of space, are defined according to the formula

$$\text{Sens}(T; \varepsilon_i) = \varepsilon_i \frac{\partial T}{\partial \varepsilon_i}, \quad \text{for } i = \overline{1, 3} \quad (10)$$

where  $T$  can be either the pressure or hydraulic flux measured along the boundaries and  $\varepsilon_i$ , for  $i = \overline{1, 3}$ , denote  $K_{11}$ ,  $K_{12}$  and  $K_{22}$ , respectively. A much enhanced characterisation of the degree of uncorrelation of the sensitivity coefficients can be viewed by calculating their ratios. We approximate the partial derivatives  $\frac{\partial T}{\partial \varepsilon_i}$  by using forward finite differences and calculate the sensitivity ratios  $R(T; \varepsilon_i, \varepsilon_j)$ , which is defined as the ratio of the sensitivity coefficients  $\text{Sens}(T; \varepsilon_i)$  and  $\text{Sens}(T; \varepsilon_j)$ .

We consider a modified least squares functional,  $LS$ , defined according to

$$LS = \left[ \alpha + \sum_{i=1}^l \sum_{j=1}^{N_{T_i}} \frac{1}{\alpha_{T_j^i}} \left[ (T_j^i)^{\text{calc}} - (T_j^i)^{\text{orig}} \right]^2 \right]^{-1} \quad (11)$$

where  $l$  is the total number of pressure or hydraulic flux measurements, the superscripts (calc) and (orig) denote the BEM numerically predicted and the simulated or measured data values, respectively, and we record  $N_{T_i}$  data measurements  $T_j^i$ , for  $i = \overline{1, l}$ , where  $T_j^i$  can denote a pressure or hydraulic flux value. Furthermore, for each  $j = \overline{1, N_{T_i}}$ , the normalising factor  $\alpha_{T_j^i}$  is chosen as a representative value of the measurement  $T_j^i$  to ensure a valid comparison between quantities of different orders of magnitude. The constant  $\alpha = 10^{-8}$  was chosen to be small enough so that significant errors in the sums of the squared differences are always sufficiently larger than  $\alpha$ .

##### 4.2.2 GA Formulation for the Inverse Problem

An improved GA based optimisation technique is employed to search in an *a priori* specified range for each of the parameters

$K_{11}$ ,  $K_{12}$  and  $K_{22}$  and the fitness function is given by the *LS* functional shown in Eq. 11. The GA process for the identification of the elements of the hydraulic conductivity tensor begins by randomly constructing an initial population of  $N$  chromosomes, each of which characterises estimates to the solution of the problem through their separate genes. The genes represent encodings of the unknown material properties over some specified ranges. We employ  $k$ -Tournament Selection, with associated probability  $p_T$ , and the fitness evaluation function 11 which measures the accuracy of the predicted pressure and/or hydraulic flux values against some known (simulated or experimental) measurements. Two-Point Crossover, with associated probability  $p_c$ , and mutation, with associated probability  $p_m$ , are used to derive child chromosomes and form a pool of offspring of size  $M$ . The  $n_e$  fittest individuals from the parent population are retained for the next generation. These steps are repeated either for a specified number of generations or until a match to the imposed data is achieved to within a desired tolerance.

### 4.3 Numerical Results and Discussion

The bounds of the chosen domain  $D = [0.75, 1.5] \times [0.25, 0.74] \times [0.75, 1.5]$  in which the search for the unknown elements of the hydraulic conductivity tensor is undertaken ensure the ellipticity of the governing partial differential equation for any triplet  $(K_{11}, K_{12}, K_{22}) \in D$  (i.e.  $K_{11}K_{22} > K_{12}^2$ ) and also include the values of the coefficients of the hydraulic conductivity tensor to be retrieved. There are only very general guidelines as to how to choose the values of the GA parameters defined in Section 4.2.2. The typical values  $N = 50$ ,  $M = 60$ ,  $p_m = 0.02$ ,  $p_c = 0.65$ , tournament pool size  $k = 2$ ,  $p_T = 0.8$  and  $n_e = 2$ , which are maintained throughout this study, have been chosen based upon experimentation on a related problem as considered in Mustata, Harris, Elliott, Ingham, and Lesnic (1999).

The estimates of  $K_{11}$ ,  $K_{12}$  and  $K_{22}$  recovered are accurate to within 0.01% for the case of specifying additional exact boundary measurements and to within 0.1% for the case of added noise. However, it is unclear whether such success can be replicated when a parameter study of a larger three-dimensional  $K_{11}$ ,  $K_{12}$  and  $K_{22}$  space is undertaken. In general, the parameter space may contain regions in which the ellipticity of the governing partial differential equation is not preserved and methods would need to be developed to overcome this. Further, if it is not possible, then it will be difficult to relate the regions of failure to the understanding of the parameter values. Hence, despite the present success, from now on the representation of the hydraulic conductivity tensor is replaced by its diagonal form when related to axes along its principal directions. Hence  $K_{11}$ ,  $K_{12}$  and  $K_{22}$  will be expressed in terms of the principal values of the stress tensor, namely  $K_1$  and  $K_2$ , with the direction of  $K_1$  making an angle  $\theta$  with the  $x_1$ -axis and also  $K_1 > K_2 > 0$ .

## 5 Problem Description

In conventional laboratory measurements, rock samples are cylindrical in shape and therefore, in two-dimensions, they can be represented as rectangles or, for simplicity, squares. A steady state flow is forced through the sample by applying constant pressures  $p_0$  and  $p_0 - \delta p_0$  on opposite faces. Transient or periodic boundary conditions can also be employed but they are not considered in this paper. The sides of the samples are jacketed with impermeable material. The boundary and initial conditions corresponding to the 2D hydraulic conductivity measurements are as follows

$$p|_{x_1=0} = p_0 \quad \forall t > 0 \quad (12)$$

$$p|_{x_1=L} = p_0 - \delta p_0 \quad \forall t > 0 \quad (13)$$

$$\left. \frac{\partial p}{\partial v^+} \right|_{x_2=0} = \left. \frac{\partial p}{\partial v^+} \right|_{x_2=L} = 0 \quad \forall t > 0 \quad (14)$$

$$p(x_1, x_2)|_{[0,L] \times [0,L]} = p_0^i \quad t = 0 \quad (15)$$

where  $L$  is the sample length and width,  $p_0^i$  is the initial pore pressure inside the sample and  $\delta p_0$  is the constant pressure difference suddenly applied across the sample at  $t = 0$  and maintained thereafter.

The governing equation is the equation of single phase flow in a two dimensional anisotropic, homogeneous, porous medium as given by Eq. 3.

## 6 The Steady State Situation

In the steady state situation, i.e.  $t \rightarrow \infty$ , the governing partial differential equation given by Eq. 3 takes the form

$$\sum_{i,j=1}^2 K_{ij} \frac{\partial^2 p}{\partial x_i \partial x_j} = 0 \quad \text{for } (x_1, x_2) \in [0, L] \times [0, L] \quad (16)$$

subject to the boundary conditions 12 – 14

### 6.1 Non-dimensional Equations

Before performing the numerical calculations, the governing equation given by Eq. 16 and the boundary conditions 12–14 are non-dimensionalised according to

$$\bar{x}_1 = \frac{x_1}{L}, \quad \bar{x}_2 = \frac{x_2}{L}, \quad \bar{p} = \frac{p - p_0 + \delta p_0}{\delta p_0}, \quad \bar{K}_{ij} = \frac{K_{ij}}{K^*} \quad (17)$$

where  $K^*$  is a typical value of the hydraulic conductivity, and hence take the following form

$$\sum_{i,j=1}^2 \bar{K}_{ij} \frac{\partial^2 \bar{p}}{\partial \bar{x}_i \partial \bar{x}_j} = 0 \quad (18)$$

$$\bar{p}|_{\bar{x}_1=0} = 1 \quad (19)$$

$$\bar{p}|_{\bar{x}_1=1} = 0 \quad (20)$$

$$\left. \frac{\partial \bar{p}}{\partial v^+} \right|_{\bar{x}_2=0} = \left. \frac{\partial \bar{p}}{\partial v^+} \right|_{\bar{x}_2=1} = 0 \quad (21)$$

where the bars have been dropped for simplicity.

## 6.2 Direct Analysis

In the direct problem formulation, provided that values for the elements of the hydraulic conductivity tensor, namely  $K_{11}$ ,  $K_{12}$  and  $K_{22}$ , are chosen so as to preserve the ellipticity of the differential operator, i.e.  $\det(\mathbf{K}) = K_{11}K_{22} - K_{12}^2 > 0$ , a boundary element method is employed in order to provide simultaneously the unspecified boundary pressure and hydraulic flux values. The relationship between the principal values of the hydraulic conductivity tensor and the elements of the hydraulic conductivity tensor relative to  $x_1$  and  $x_2$  axes are as follows

$$K_{11} = K_1 \cos^2 \theta + K_2 \sin^2 \theta, \quad (22)$$

$$K_{12} = K_{21} = (K_1 - K_2) \cos \theta \sin \theta, \quad \text{and} \quad (23)$$

$$K_{22} = K_2 \cos^2 \theta + K_1 \sin^2 \theta. \quad (24)$$

Note that in the reference frame  $x_1, x_2, x_3$ , where  $x_3$  is assumed to correspond to the direction of the principal hydraulic conductivity  $K_3$ , the flow equations do not depend on  $x_3$  and the problem can be considered to be two-dimensional.

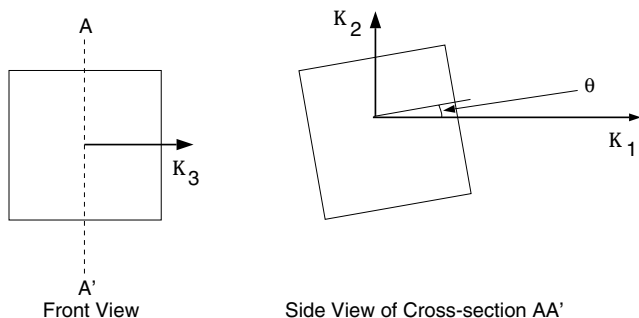


**Figure 1** : An illustration of the anisotropic material with the hydraulic conductivity ratio  $K_2/K_1 = 0.2$ . The  $x_1$ -axis of the sample is inclined at the angle  $\theta$  to the direction of the maximum principal hydraulic conductivity  $K_1$ .

As mentioned earlier, rather than providing the elements of the hydraulic conductivity tensor we provide the magnitude of the principal hydraulic conductivities, which are initially fixed to the ratio  $K_2/K_1 = 0.2$ , together with various values for the angle  $\theta$  that the  $x_1$ -axis of the sample makes with the direction of the maximum principal value  $K_1$  as shown in Fig. 1. The non-dimensional principal hydraulic conductivity values are chosen to be, for simplicity,  $K_2 = 1$  and  $K_1 = 5$ .

Pressure and hydraulic flow distributions along the boundaries at which they were not specified have been compared for various numbers of boundary elements ranging from 40 to 160. No significant differences in the results obtained were observed except in the vicinity of the corners. However, such values

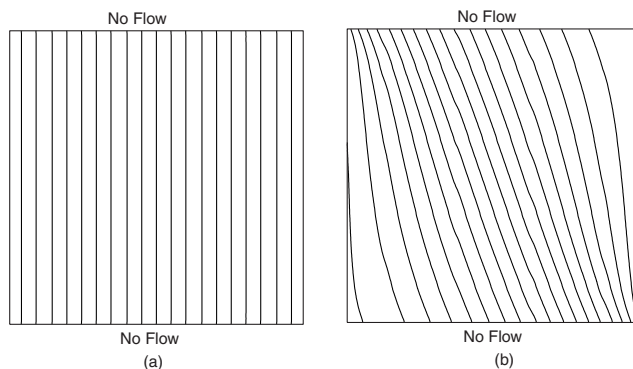


**Figure 2** : Pressure contours in the sample with the hydraulic conductivity ratio  $K_2/K_1 = 0.2$  and the orientation of the principal direction such that (a)  $\theta = 0^\circ$  and (b)  $\theta = 60^\circ$ . The contours indicate pressure values  $p = 1(0.05)0$  from the upstream to the downstream face of the sample.

will not be used in the inversion technique which will be undertaken later in this paper.

Examples of the steady state simulated pressure fields inside the sample are presented in Fig. 2 and we can observe that the pressure gradient is constant inside the sample in (a), which is equivalent to a one-dimensional flow through the rock sample, whereas in the second case, namely (b), the pressure field is strongly distorted due to the presence of the impermeable jacket. The latter conclusion remains valid for other angles within the range  $\theta \in [0^\circ, 90^\circ]$  except those close to the limits of the above mentioned interval when the flow becomes almost one-dimensional.

In general, the flow patterns inside the sample for a given orientation  $\theta$  are also distorted and examples of these are shown in Fig. 3.

The orientation of the maximum principal hydraulic conductivity value varies from being aligned with the sample  $x_1$ -axis, as in Fig. 3 (a), to being along the diagonal from the top left hand corner of the sample to the bottom right hand corner, as in Fig. 3 (c), and this causes the direction of the flow to respond in a similar manner. Hence as the angle  $\theta$  increases from  $0^\circ$  to  $60^\circ$ , the flow direction in the upper left hand corner and in the lower right hand corner change from being horizontal to follow the principal direction related to the maximum principal value of the hydraulic conductivity tensor. However, the no flow conditions on the boundaries  $x_2 = 0$  and  $x_2 = 1$  prevent this type of flow from continuing into the corners of the sample where the flow is strongly influenced by the boundaries.

## 6.3 Inverse Formulation

A number of methods have been proposed to measure the full hydraulic conductivity tensor in rocks or soils. Fontugne (1969) performed two flow measurements simultaneously on

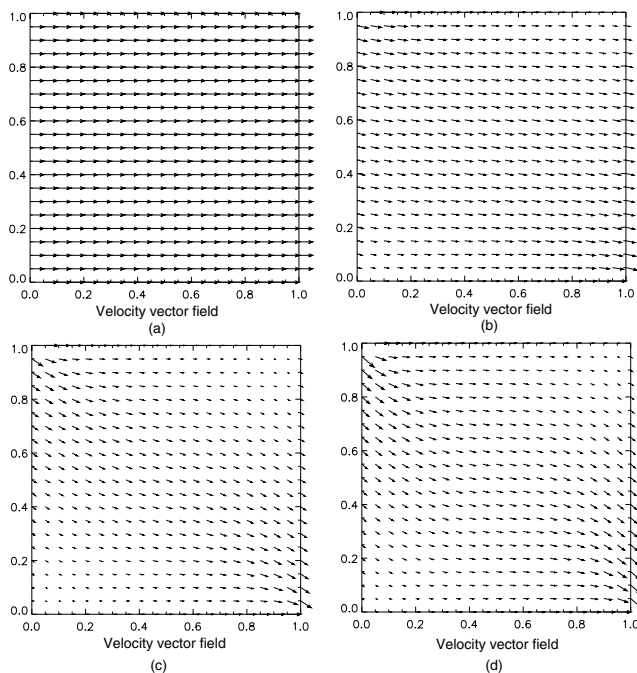


**Figure 3** : Flow patterns in the sample with the hydraulic conductivity ratio  $K_2/K_1 = 0.2$  and the direction of the maximum principal value such that (a)  $\theta = 0^\circ$ , (b)  $\theta = 15^\circ$ , (c)  $\theta = 45^\circ$ , and (d)  $\theta = 60^\circ$ .

a prepared soil, with the fluid outlets aligned with the assumed principal directions, and then determined the ratio of the principal hydraulic conductivities. The amplitudes of the principal hydraulic conductivities were measured separately. Rose (1970) designed an experimental procedure to force the stream lines to be straight lines parallel to the sample axis. However, this method involves the re-shaping, by trial and error, of the sample, making it difficult to implement in practice. All of these methods assume that the sample axis can be oriented parallel or perpendicular to one of the principal directions, which is not as serious a restriction as it might appear since, in many cases, at least one of the principal directions can be guessed from the bedding planes preferred orientation of the micro-cracks and the like. The commonly used concept of horizontal and vertical hydraulic conductivities implicitly assumes that the principal hydraulic conductivity directions in-situ are likewise, but this is not always true. However, samples can be taken in directions parallel and perpendicular to the bedding planes when visible, rather than parallel and perpendicular to the axis of the core as it is usually done.

If the principal directions cannot be estimated, a different method becomes necessary. The best solution would be to measure the full hydraulic conductivity tensor in one single sample by imposing periodic boundary conditions as considered by Quintard and Whitaker (1987), Saez, Otero, and

Rusinek (1989), Mei and Auriault (1989), and Durlofsky and Chung (1987). Whilst this can be achieved, it is rather difficult to implement in practice. Alternatively, it may be possible to perform a suite of independent flow measurements, each one with a different set of Neumann and Dirichlet boundary conditions. As this is perfectly possible in laboratory measurements this method may yield enough information to allow one to infer the full hydraulic conductivity tensor. A similar idea was applied by White and Horne (1987), but in another context. Bernabe (1992) sketched a possible procedure involving six steady state flux measurements (two longitudinal, and the rest diagonal) and inferred the components of the hydraulic conductivity tensor with an accuracy that varied from 10% for the largest tensor component to 30% for the smallest.

The inverse analysis requires the identification of the values of the principal hydraulic conductivities  $K_1$  and  $K_2$  and the angle between the direction of the maximum principal value of the hydraulic conductivity tensor and the horizontal direction of the sample, namely  $\theta$ , only from local measurements of the pressure and/or average hydraulic flux on the boundary of the rock sample. Therefore, in practice, possible reliable measurements involve pressure readings on the bottom and top face of the sample and flux readings at the downstream or upstream faces of the rock sample, since in the steady state case the average fluxes on the downstream and upstream faces of the sample are the same. Hence, we consider a modified least square functional,  $LS$ , defined in a similar manner as shown in Eq. 11, which depends upon the pressure and/or average hydraulic flux values, rather than the pressure and local flux values as before.

The GA based optimisation technique described in Section 4.2.2, together with the values for the evolution parameters given in Section 4.3, is employed to search in an *a priori* specified range for each of the parameters  $K_1$ ,  $K_2$  and  $\theta$ , where the fitness function is given by Eq. 11 with the above mentioned modifications.

## 7 Numerical Results and Discussion for the Steady State Situation

The ranges for the unknown parameters defining the domain of search for the GA optimisation are given by  $(K_1, K_2, \theta) \in D = [1, 10] \times [0.25, 1.75] \times [0^\circ, 90^\circ]$ . The range for the angle is dictated by the fact that for  $90^\circ < \theta \leq 180^\circ$  the problem is equivalent to using an angle of  $180^\circ - \theta$  and interchanging the roles of  $K_1$  and  $K_2$ . All the numerical simulations are performed using a boundary element method with 80 boundary elements, as this number proved to be sufficiently large to render accurate simulations of the boundary data necessary in the inversion process, see Section 4. Prior to performing the inversion for the values of  $K_1$ ,  $K_2$  and  $\theta$ , it is useful to perform a sensitivity analysis of the effect of small changes in the parameters on the boundary simulated pressure and/or average hydraulic flux. The normalised sensitivity coefficients as a function of space, are defined according to Eq. 10, where  $T$

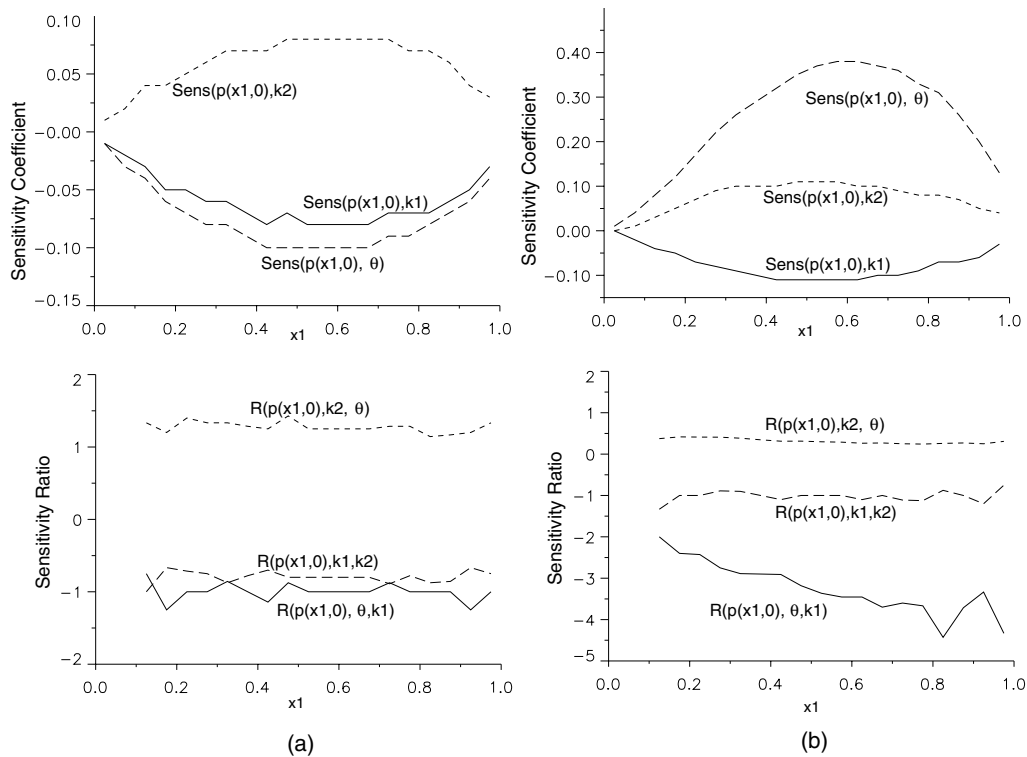


**Figure 4** : Sensitivity coefficients and sensitivity ratios with respect to pressure on the bottom face of the rock sample for the cases (a)  $\theta = 10^\circ$ , and (b)  $\theta = 60^\circ$ .

can be either the pressure or average hydraulic flux measured along the boundaries and  $\varepsilon_i$ , for  $i = \overline{1,3}$ , denote  $K_1$ ,  $K_2$  and  $\theta$ , respectively as described in Section 4.2.1.

In Fig. 7 the sensitivity coefficients, as well as their ratios, for the pressure measured along the bottom face of the sample are plotted for various angles  $\theta$ . In the case of the sensitivity coefficients, the solid and dotted lines represent the sensitivity coefficients with respect to  $K_1$  and  $K_2$ , respectively, and the dashed line represents the sensitivity coefficient with respect to the angle  $\theta$ . In the case of the sensitivity ratios, the dashed, dotted and solid lines represent the ratio of the sensitivity coefficient for  $K_1$ , to the sensitivity coefficient for  $K_2$ , the ratio of the sensitivity coefficient for  $K_2$ , to the sensitivity coefficient for  $\theta$  and the ratio of the sensitivity coefficient for  $\theta$ , to the sensitivity coefficient for  $K_1$ , respectively. It can be seen that the smaller the value of the angle  $\theta$  the smaller is the sensitivity of the pressure with respect to the angle. This means that measurements of the pressure alone do not provide sufficient information to fully retrieve the unknown values of the principal hydraulic conductivities  $K_1$  and  $K_2$  and the angle  $\theta$ , but just the ratio of  $K_1$  and  $K_2$  and the angle  $\theta$ . However, difficulties can be encountered in retrieving even these parameters when the angle is close to the limits of the interval  $[0^\circ, 90^\circ]$  due to the low sensitivity of the pressure for such angles. This can also be argued from the mathematical formulation of the model since on dividing the governing equation and boundary

conditions by one of the elements of the hydraulic conductivity tensor we obtain an equivalent problem that is dependent upon only two parameters, namely the ratio of the components of the hydraulic conductivity tensor, or, in our case, the ratio of its principal values and the angle  $\theta$ . This is contrary to the situation in Section 4 where the test example involved a non zero flux on the boundaries  $x_2 = 0$  and  $x_2 = 1$  which avoided the non-uniqueness of the problem as regards the ratio of the principal hydraulic conductivity values.

We attempt to use the average value of the hydraulic flux on the downstream face of the sample rather than the pointwise values of the flux based upon practical considerations, such a quantity being easier to measure. The sensitivity of the average flux on the downstream face of the sample was found to have a similar behaviour to the sensitivity of the pressure with respect to the angle, namely the smaller the value of the angle  $\theta$  the smaller is the sensitivity of the average hydraulic flux with respect to any of the three unknowns  $K_1$ ,  $K_2$  or  $\theta$ . In addition, for any angle the sensitivity coefficients for  $K_1$  and  $K_2$  are correlated, whereas the other two remaining pairings of sensitivity coefficients are uncorrelated.

Due to the above non-uniqueness of the inversion process when using only pressure measurements, and the fact that average flux at a given angle  $\theta$  provides only a single value for the inversion process, it is proposed to investigate the situation

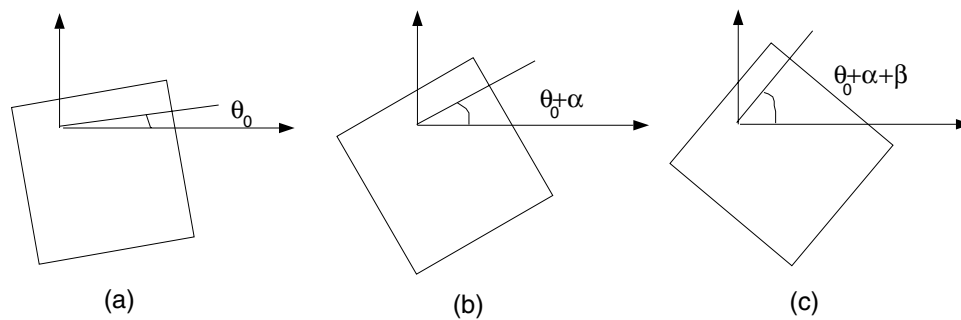


**Figure 5** : Example of different configurations obtained by cutting samples at (a)  $\theta_0$ , (b)  $\theta_0 + \alpha$ , and (c)  $\theta_0 + \alpha + \beta$ .

where additional flux measurements can be made available by taking different values of  $\theta$ . If  $\theta_0$  denotes the unknown angle between the direction of the maximum principal value of the hydraulic conductivity tensor and the  $x_1$ -axis of the sample, then we consider the orientations  $\theta_0 + \alpha$  and  $\theta_0 + \beta$ , where  $\alpha$  and  $\beta$  are known values. Hence it is proposed for the following analysis that samples are to be cut from the rock specimen and from such experiments additional sets of pressure readings and average flux measurements will be available whilst the unknown parameters to be determined, namely  $K_1$ ,  $K_2$  and  $\theta_0$ , remain the same.

### 7.1 Average Flux Measurements Only

When using only average flux measurements we consider three configurations, i.e. the  $x_1$ -axis of the sample is cut at the unknown angle  $\theta_0$  from the direction of the principal value  $K_1$  of the hydraulic conductivity tensor and the other two configurations are obtained by cutting samples under the angles  $\alpha$  and  $\alpha + \beta$ , with  $\alpha < \beta$ , from the original angle  $\theta_0$ , as shown in Fig. 7.1. This is equivalent to rotating the  $x_1$ -axis of the sample along which the imposed pressure difference is applied from the original angle  $\theta_0$  by the angles  $\alpha$  and  $\alpha + \beta$  in an anti-clockwise direction, respectively. The angles  $\alpha$  and  $\beta$  are considered to be known quantities, whereas  $\theta_0$  is sought along with the principal hydraulic conductivities of the sample, namely  $K_1$  and  $K_2$ . Any fewer configurations, i.e. less number of cuts, will not provide sufficient information as in the steady state the average fluxes at both ends of the sample are identical and hence only one piece of information is provided from each configuration.

After considering different magnitudes of rotation in the range  $[15^\circ, 60^\circ]$  for various original angles  $\theta_0$  we chose the values  $\alpha = \beta = 45^\circ$  to perform the inversion. In the first instance, the restricted range  $R = [2, 7] \times [0.25, 1.75] \times [0^\circ, 20^\circ]$  was considered in order to retrieve the values  $(K_1, K_2, \theta) = (5, 1, 10^\circ)$ . The characteristic results obtained were accurate to within 0.01% for the values of the principal hydraulic conductivities and 1.5% for the angle  $\theta_0$  with a typical solution from the GA inversion technique having the form  $(K_1, K_2, \theta) = (5.0059, 1.0095, 10.127^\circ)$ . However, when enlarging the do-

main to the aforementioned domain  $D$  the algorithm failed to render a very accurate estimation of the unknowns with typical values having the form  $(K_1, K_2, \theta) = (4.9326, 1.0433, 8.798^\circ)$ . Based on the observed behaviour that the GA reaches values close to the optimal ones after a fairly small number of iterations we can employ an automatic technique of ‘shrinking’ the range based on successive runs of the GA in order to continuously improve the accuracy of the estimates of the required parameter values. Taking the last  $n$  fittest individuals in the previous run of the GA and calculating their mean, minimum and maximum values, a new range is constructed with this mean at its centre value. The new range is 1/4 of the size of the original range but is additionally self contained in the previous range. In this way we obtain a descending array of ranges in which the GA does its search and, providing the binary representation of the solution stays the same, the accuracy will increase as shown in Tab. 1 and Tab. 2. This process was tested for values of  $n$  ranging from 10 to 30 but no significant improvements have been observed in the retrieved values for the unknown parameters.

**Table 1** : Results of the GA recovery of the principal hydraulic conductivities and the angle  $\theta_0$  when employing the reduction of the ranges technique.

	Run1	Run2	Run3
$K_1$	5.1437	4.9411	5.0008
$K_2$	1.0550	0.9948	0.9999
$\theta_0$	12.669°	8.883°	10.008°

Typical results of the recovery of the unknown principal hydraulic conductivities and the angle are presented after two successive reductions of the range. It can be seen that the results gain in accuracy at every reduction of the range and by this technique we can obtain results which are virtually as accurate as we desire. Thus, by combining the GA optimisation scheme with the reduction of the range technique we can obtain accurate results when using just average fluxes in three configurations. However, there are some drawbacks to

**Table 2** : Corresponding reduced ranges for consecutive runs of the GA.

Ranges1	Ranges2	Ranges3
[1.0, 10.0]	[3.98, 6.23]	[4.66, 5.22]
[0.25, 1.75]	[0.86, 1.24]	[0.95, 1.04]
[0.0°, 90.0°]	[1.56°, 24.06°]	[6.07°, 11.70°]

this technique and these are mainly from a practical point of view, namely it may be physically unrealistic to provide three samples with identical properties for different configurations.

## 7.2 Pressure and Average Flux. Two steps

In this section we return to a single configuration, i.e. one cut, and the information that we use for inversion is given by the boundary pressure measurements on the bottom face of the sample and the average hydraulic flux value on the downstream face of the sample. We aim to use minimal information in order to retrieve the principal hydraulic conductivities  $K_1$  and  $K_2$  and the angle that the  $x_1$ -axis of the sample makes with the direction of the maximum principal hydraulic conductivity value, namely  $\theta_0$ . This will come in the form of two pressure readings combined with the average flux. As discussed in the sensitivity analysis performed at the beginning of the Section 7, pressure readings alone will not provide sufficient information to fully retrieve  $K_1$ ,  $K_2$  and  $\theta_0$  since only the ratio  $K_1/K_2$  and  $\theta_0$  can be retrieved. Also the closer the angle is to the limits of the range  $[0^\circ, 90^\circ]$ , the less is the pressure response to small changes in the angle and therefore it is highly improbable that the value of the angle can be retrieved accurately. However, when using **only pressure readings** in the inversion we can employ the same sort of ‘shrinking’ technique for the ranges, as discussed earlier, in order to obtain accurate results for both the ratio of the principal hydraulic conductivities  $K_1/K_2$  and the angle  $\theta_0$  no matter at what angle the sample is cut. Having found the ratio  $K_1/K_2$  and the angle  $\theta_0$  accurately we have several options to fully retrieve all the unknowns:

- (i) We can cut the sample such that the  $x_1$ -axis is along the direction corresponding to the maximum principal value of the hydraulic conductivity, namely  $\theta_0 = 0^\circ$ , and then the problem is one-dimensional only. We can then apply Darcy’s law and fully determine the remaining pair of unknowns, namely the principal hydraulic conductivities  $K_1$  and  $K_2$ , since the ratio  $K_1/K_2$  is known.
- (ii) Alternatively, in the same configuration we can fix the value of the angle to be the one retrieved in the first step and then continue the inversion by using as additional information the average hydraulic flux value on the downstream face of the sample.

It is this latter approach that is illustrated in the following. Three pressure measurements, chosen according to the sensitivity analysis as the positions in which the pressure is most sensitive to changes in the parameters, will provide the information used in the inversion in the first step. Tab. 3 shows

**Table 3** : Results of the GA recovery of the ratio of the principal permeabilities and the angle  $\theta_0$  when employing the reduction of the ranges technique in the case of using three pressure measurements

	Run1	Run2	Run3	Run4
Ratio	5.64	5.19	5.05	5.00
$\theta_0$	9.06°	9.70°	9.91°	9.99°

typical results of the GA optimisation scheme combined with the reduction of the range and we can see that at each step both the value of the ratio of the principal hydraulic conductivities and the angle  $\theta_0$  are heading towards their exact values. Then on fixing the value of the angle at  $\theta_0 = 9.99^\circ$  and adding into the inversion process as supplementary information the average hydraulic flux value on the downstream face of the sample, we obtain accurate estimates for the principal hydraulic conductivities, namely  $(K_1, K_2) = (5.0029, 0.9902)$ .

## 8 Conclusions

The present research has established that by combining a BEM method for the direct approach with an inversion technique based upon Genetic Algorithm evolution principles we obtain a feasible technique for identifying the unknown hydraulic conductivity tensor  $\mathbf{K}$  of anisotropic materials, although a successful retrieval of these parameters depends both on the dependent variable measured and the configuration at which their values are recorded. A successful retrieval of the elements of the hydraulic conductivity tensor when using additional average flux measurements alone is subject to the use of three different configurations, but this approach has practical drawbacks. When considering a single configuration, the inversion process has to be performed in two steps and both pressure values and average flux values are required to fully retrieve the unknown hydraulic rock properties.

**Acknowledgement:** R. Mustata is grateful to the ORS research scheme as well as to the Department of Applied Mathematics at University of Leeds for the funding of this research.

## References

**Begg, S. H.; Carter, R. R.; Dranfield, P.** (1989): Assigning effective values to simulate gridblock parameters for heterogeneous reservoirs. SPE Reservoir Eng., vol. 4, pp. 455–463.

- Bernabe, Y.** (1992): On the measurement of permeability in anisotropic rocks. In *Fault Mechanics and Transport Properties of Rocks*, pp. 147–167. Academic Press Ltd.
- Brebbia, C. A.; Telles, J. C. F.; Wrobel, L. C.** (1984): *Boundary Element Techniques: Theory and Application in Engineering*. Springer-Verlag, Berlin.
- Chang, Y. P.; Kang, C. S.; Chen, D. J.** (1973): The use of fundamental Green's functions for the solution of problems of heat conduction in anisotropic media. *J. Heat Mass Transfer*, vol. 16, pp. 1905–1918.
- Dagan, G.** (1986): Statistical theory of groundwater flow and transport: pore to laboratory, laboratory to formation and formation to regional scale. *Water Resources Res.*, vol. 22(9), pp. 120S–134S.
- Durlofsky, L. J.; Chung, E. Y.** (1987): Effective permeability of heterogeneous reservoir regions. In *2nd European Conf. on Math. of Oil Recovery*, pp. 57–64, Paris. Editions Techniq.
- Fontugne, D. J.** (1969): Permeability measurement in anisotropic media. Master's thesis, Syracuse University, 1969.
- Hewett, T. A.; Behrens, R. A.** (1990): Considerations affecting the scaling of displacements in heterogeneous permeability distributions. *65th Ann. Tech. Conf., New Orleans, SPE paper 20575*, 1990.
- Lake, L. W.** (1988): The origins of anisotropy. *J. Pet. Tech.*, vol. 40, pp. 395–396.
- Mei, C. C.; Auriault, J.-L.** (1989): Mechanics of heterogeneous porous media with several spatial scales. *Proc. R. Soc. London*, vol. A426, pp. 391–423.
- Mustata, R.; Harris, S. D.; Elliott, L.; Ingham, D. B.; Lesnic, D.** (1999): Parameter investigation in a Boundary Element Model of a hydraulic pump test. In *Boundary Element Techniques*, pp. 331–340.
- Quintard, M.; Whitaker, S.** (1987): Ecoulement monophasique en milieu poreux: effet des heterogeneites locales (in french). *J. Meca. Theor. Appl.*, vol. 6(5), pp. 691–726.
- Rice, P. A.; Fontugne, D. J.; Latini, R. G.; Barduhn, A. J.** (1970): Anisotropic permeability in porous media. *Ind. Eng. Chem.*, vol. 62, pp. 23–31.
- Rose, W. D.** (1970): New method to measure directional permeability. *J. Pet. Tech.*, vol. 34, pp. 1142–1144.
- Saez, A. E.; Otero, C. J.; Rusinek, I.** (1989): The effective homogeneous behavior of heterogeneous porous media. *Transport in Porous Media*, vol. 4, pp. 213–238.
- Sternberg, W. J.; Smith, T. L.** (1946): *The Theory of Potential and Spherical Harmonics*. University of Toronto Press, Toronto.
- Symm, G. T.; Pitfield, R. A.** (1974): Solution of Laplace's equation in two dimensions. *NAC 44, NPL Report*, 1974.
- White, C. D.; Horne, R. N.** (1987): Computing absolute transmissibility in the presence of fine-scale heterogeneity. *SPE Symp. on Reservoir Simulation, San Antonio, SPE paper*, 1987.